AIAA JOURNAL
Vol. 45, No. 2, February 2007

Technical Notes

TECHNICAL NOTES are short manuscripts describing new developments or important results of a preliminary nature. These Notes should not exceed 2500 words (where a figure or table counts as 200 words). Following informal review by the Editors, they may be published within a few months of the date of receipt. Style requirements are the same as for regular contributions (see inside back cover).

Dragonfly Forewing–Hindwing Interaction at Various Flight Speeds and Wing Phasing

Hua Huang* and Mao Sun†
Beijing University of Aeronautics and Astronautics, 100083 Beijing, People's Republic of China

DOI: 10.2514/1.24666

I. Introduction

DRAGONFLIES are accomplished fliers. Scientists have always been fascinated by their flight. Experimental and computational studies on a single airfoil in dragonfly hovering mode were conducted by Freymuth [1] and Wang [2], respectively. They showed that large vertical force was produced during each downstroke. In each downstroke, a vortex pair was created; the large vertical force was explained by the downward two-dimensional jet induced by the vortex pair [2]. Recently, due to the advances in computational and experimental techniques and facilities, researchers are beginning to study dragonfly aerodynamics and forewing–hindwing interactions using three-dimensional model wings [3–5]. Sun and Lan [3] studied the aerodynamics and the forewing–hindwing interaction of a dragonfly in hover flight, using the method of computational fluid dynamics (CFD). Maybury and Lehmann [4] and Yamamoto and Isogai [5] conducted experimental studies on the forewing–hindwing interaction at hovering conditions. Wang and Sun [6] extended the computational study of Sun and Lan [3] to the case of forward flight. In most of these studies, only hovering flight was considered. Only Wang and Sun [6] investigated the effects of forward flight speed, but the investigation was limited to a few phase differences ($\gamma_d = 0$, 60, 90, and 180 deg; γ_d denotes the difference in phase angle between the forewing and the hindwing stroke cycles, positive when the hindwing leads the forewing and negative when the forewing leads the hindwing). Because the distance of a wing from the wake of another wing depends on the flight speed and the relative motion of the fore- and hindwings, it is expected that the forewing–hindwing interaction is strongly influenced by the flight speed and the relative phase difference. Therefore, it is desirable to study the forewing–hindwing interaction by systematically varying the flight speed and the phase angle. Moreover, in the above studies [3–6], attention was mainly paid on whether or not the aerodynamic forces were changed by the forewing–hindwing interaction, while how the interaction occurred was not well understood. It is of interest to make further investigation on the flow field of the wing wake to reveal how the forewing–hindwing interaction occurs.

Received 17 April 2006; revision received 7 September 2006; accepted for publication 19 September 2006.

*Graduate Student, Institute of Fluid Mechanics.
†Professor, Institute of Fluid Mechanics; m.sun@263.net.

In the present study, we address the above questions by numerical simulation of the flows of model dragonfly wings. The phasing and the flight speed are systematically varied. Advance ratio (the nondimensional flight speed) ranges form 0 to 0.6. At each advance ratio, eight phase differences, −180, −135, −90, −45, 0, 45, 90, and 135 deg, are considered.

II. Methods

In the present study, we use the same wing planform for both the model wings (Fig. 1a). The planform is similar to that of the forewing of *Aeshna juncea* [7]. The thickness of the wings is 1% of c (where c is the mean chord length of the wing). The radius of the second moment of wing area (denoted by r_2) is $r_2 = 0.61R$, where R is the wing length. The flapping motions of the wings are shown in Fig. 1b. The freestream velocity, which has the same magnitude as the flight velocity, is denoted by V_∞, and the stroke plane angle is denoted by β. The wing flaps downward and upward along the stroke plane and rotates during stroke reversal (Fig. 1b). For a detailed description of the flapping motion see Wang and Sun [6]. The advance ratio (J) is defined as $J = V_\infty/(2\Phi nR)$, where Φ and n are the stroke amplitude and stroke frequency of the wing, respectively. The kinematic parameters, which determine the wing motion, are the same as that used in Wang and Sun [6], except that more phase difference (γ_d) between forewing and hindwing and more downstroke (α_d) and upstroke (α_u) angles of attack are considered here.

The incompressible unsteady Navier–Stokes equations are numerically solved using moving overset grids. The Reynolds number $Re = Uc/\nu$, where U is the mean flapping velocity ($U = 2\Phi nr_2$) and ν the flow viscosity, is 1470. The computational method has been described in detail in Sun and Lan [3] and Sun and Yu [8] and will not be repeated here. To test the grid resolution, the flows at hovering ($J = 0$) and at the maximum advance ratio considered in the present study ($J = 0.6$) were computed, using two grid systems, grid system 1 and grid system 2. In both grid systems, the outer boundary of the wing grid was set at about $2c$ from the wing surface and that of the background grid at about $40c$ from the wings. For grid system 1, the wing grid had dimensions $29 \times 77 \times 45$ in the normal direction, around the wing, and in the spanwise direction, respectively, and the background grid had dimensions $90 \times 72 \times 46$ in the X (horizontal), Z (vertical), and Y directions, respectively. For grid system 2, the corresponding grid dimensions were $58 \times 157 \times 91$ and $165 \times 118 \times 85$. The first layer grid thickness for grid system 1 is $0.0003c$, and for grid system 2, $0.0002c$. For both grid systems, grid points of the background grid concentrated in the near field of the wings where its grid density was approximately the same as that of the outer part of the wing grid. There was almost no difference between the force coefficients calculated by the two grid systems. It was concluded that grid system 1 was appropriate for the present study. The effect of time step value was considered and it was found that a numerical solution effectively independent of the time step was achieved if $\Delta\tau \leq 0.02$. Therefore, $\Delta t = 0.02$ was used in the present calculations.

Resolving the aerodynamic force of a wing into the Z and X axes (Fig. 1b) gives the vertical force and negative thrust of the wing. Let V_f and T_f denote the vertical force and thrust of the forewing, respectively; let V_h and T_h denote the vertical force and thrust of the hindwing, respectively. The coefficients of V_f, T_f, V_h, and T_h are denoted as $C_{V,f}$, $C_{T,f}$, $C_{V,h}$, and $C_{T,h}$, respectively. They are defined

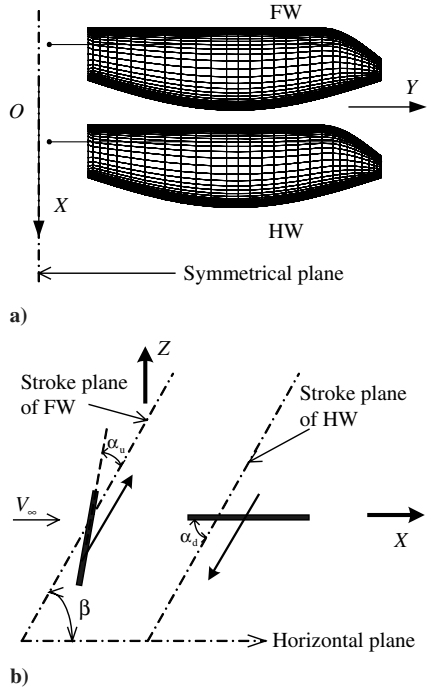

Fig. 1 The model wings and their motion (FW, forewing; HW, hindwing).

as

$$C_{V,f} = \frac{V_f}{0.5\rho U^2(2S)}, \ldots \tag{1}$$

where ρ is the fluid density and S is the area of one wing. The total vertical force (V) and total thrust (T) of the fore- and hindwings are $V = V_f + V_h$ and $T = T_f + T_h$, respectively. The coefficients of V and T are denoted as C_V and C_T, respectively, and defined as

$$C_V = \frac{V}{0.5\rho U^2(2S)} = C_{V,f} + C_{V,h} \tag{2}$$

$$C_T = \frac{T}{0.5\rho U^2(2S)} = C_{T,f} + C_{T,h} \tag{3}$$

III. Results and Discussion

A. Effects of Phase Difference and Flight Speed on the Aerodynamic Forces

Figure 2 gives the variations of the mean total vertical force coefficient ($\bar{C}_V$) and mean total thrust coefficient ($\bar{C}_T$) as functions of phase angle and advance ratio (with α_d and α_u fixed at 50 and 40 deg, respectively). To obtain quantitative data on the interaction between the fore- and hindwings, flows around a single wing that has the same motion as the forewing (or the hindwing) are also computed. The differences between the coefficients of the total vertical force and total thrust of the fore- and hindwings and their counterparts of two single wings represent the effect of the interaction (the results of the single wings are included in the figure; let $C_{V,s}$ and $C_{T,s}$ denote the vertical force and thrust coefficients of the single wing, respectively; $\bar{C}_{V,s}$ and $\bar{C}_{T,s}$ are the mean vertical force and thrust coefficients of the single wing, respectively). The main features of the results in Fig. 2 are that at positive γ_d (hindwing leads forewing), the mean total vertical force and mean total thrust are only slightly influenced by the forewing–hindwing interaction, while at negative γ_d (hindwing lags forewing), the forces, especially the mean total vertical force, are greatly decreased, compared with the case without interaction. Comparing the mean force coefficients of the forewing (or the hindwing) with its counterparts of the single wing (the figures

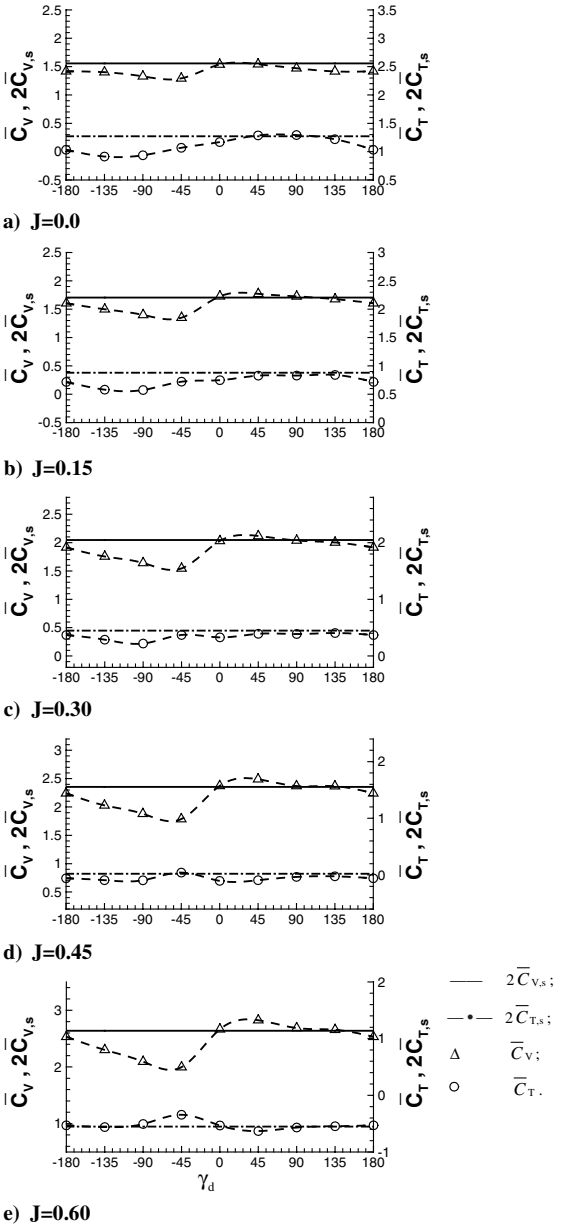

Fig. 2 Mean total vertical force and thrust coefficients.

comparing these force coefficients are not given here owing to the limitation of space) shows that the forewing is only slightly influenced by the forewing–hindwing interaction, but the hindwing is greatly influenced by the forewing–hindwing interaction at negative γ_d (in the range of γ_d from 0 to −180 deg, the vertical force coefficient of the hindwing is decreased by around 20–60%, compared with that of the single wing). The decreases in the forces of the hindwing due to the forewing–hindwing interaction result in the decreases in the mean total forces at negative γ_d shown in Fig. 2.

In the above computations for various advance ratios and phase differences, α_d and α_u are set as 50 and 40 deg, respectively. Computations have been made for other typical angles of attack ($J = 0$: $\alpha_d = 50$ deg and $\alpha_u = 8$ deg; $J = 0.15$: $\alpha_d = 44$ deg and $\alpha_u = 14$ deg; $J = 0.3$: $\alpha_d = 36$ deg and $\alpha_u = 22$ deg; $J = 0.45$: $\alpha_d = 33$ deg and $\alpha_u = 36$ deg; $J = 0.6$: $\alpha_d = 32$ deg and $\alpha_u = 51$ deg). The main features regarding the forewing–hindwing interaction are the same as that shown in Figs. 2.

B. Time Courses of the Aerodynamic Forces of Typical Cases

In the above section, mean force coefficients have been discussed. Here we examine the time courses of the force coefficients, which can

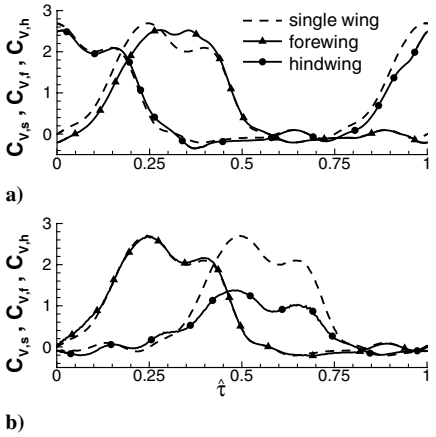

Fig. 3 Vertical force coefficients in one cycle: a) $\gamma_d = 90$ deg and b) $\gamma_d = -90$ deg.

show when the interaction occurs in a stroke cycle. As examples, we examine the results of two typical cases, one for $\gamma_d = 90$ deg and the other for $\gamma_d = -90$ deg (at $J = 0.3$, $\alpha_d = 36$ deg, and $\alpha_u =$ 22 deg). As known from above, at $\gamma_d = 90$ deg, the forewing–hindwing interaction effect is small, while at $\gamma_d = -90$ deg, it is very large.

For a clear description of the time courses of the force coefficients, we express time during a stroke cycle as a nondimensional parameter $\hat{\tau}$ such that $\hat{\tau} = 0$ at the start of the downstroke of the forewing and $\hat{\tau} = 1$ at the end of the following upstroke of the forewing. Figure 3a gives the time courses of the vertical force coefficients for the case of $\gamma_d = 90$ deg. Both the vertical force coefficients of the forewing and the hindwing are only slightly different from their counterpart of the single wing in the whole stroke cycle. Figure 3b gives the results of the case of $\gamma_d = -90$ deg. The force coefficient of the forewing is not very different from its counterpart of the single wing, while the force coefficient of the hindwing is much less than its counterpart of the single wing during the downstroke (note that for the case of $\gamma_d = -90$ deg, the hindwing lags the forewing by $\frac{1}{4}$ cycle and its downstroke is at $\hat{\tau} = 0.25$–0.75). This shows that the large detrimental effect on the hindwing at $\gamma_d = -90$ deg occurs during its downstroke (the results here are also true for other cases of negative γ_d).

C. Flow Fields of the Forewing–Hindwing Interaction

To further understand the forewing–hindwing interaction, we examine the flow fields of the wings in the above typical cases, and compare them with that of the single wing. Figure 4a shows the sectional streamline plot at half-wing length at middownstroke for the single wing; Figs. 4b and 4c show the corresponding results for the hindwing at $\gamma_d = 90$ deg and $\gamma_d = -90$ deg, respectively (the flow patterns of the forewing are not very different from their counterparts of the single wing and are not shown here).

In the case of $\gamma_d = -90$ deg (Fig. 4b), the angle between the incoming flow and the chord of the hindwing, which represents the effective angle of attack of the wing, is not very different from its counterpart of the single wing (comparing Fig. 4b with Fig. 4a).

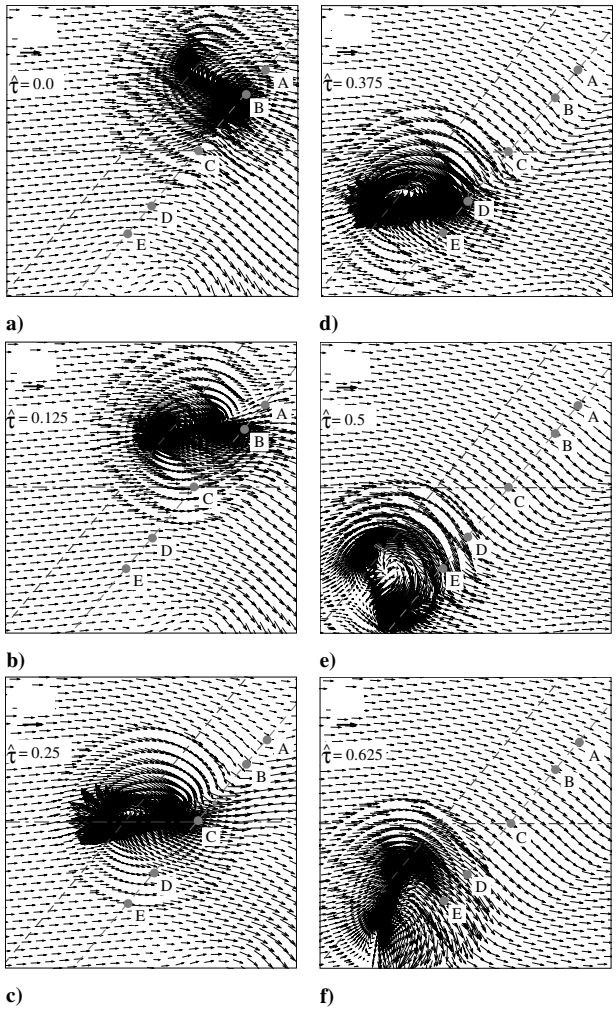

Fig. 5 Velocity vector plots (horizontal arrow at the top left represents reference velocity).

However, in the case of $\gamma_d = -90$ deg (Fig. 4c), the incoming flow is almost aligned with the wing chord; that is, the effective angle of attack of the wing is much smaller than that of the single wing (comparing Fig. 4c with Fig. 4a). This clearly shows that the interaction effect is to decrease the effective angle of attack of the hindwing, reducing its aerodynamic force (this is also true for other cases of negative γ_d).

D. Explaining the Forewing–Hindwing Interaction

Figure 5 shows the velocity vectors projected in a vertical plane that is parallel to and $0.6R$ from the plane of symmetry at various times of a cycle for the single wing. It is reasonable to expect that the velocity vector plots could approximate those of the forewing. When the forewing sweeps down in its downstroke (Figs. 5a–5e), below the wing (e.g., at points C, D, and E in Figs. 5a and 5b and at points D and

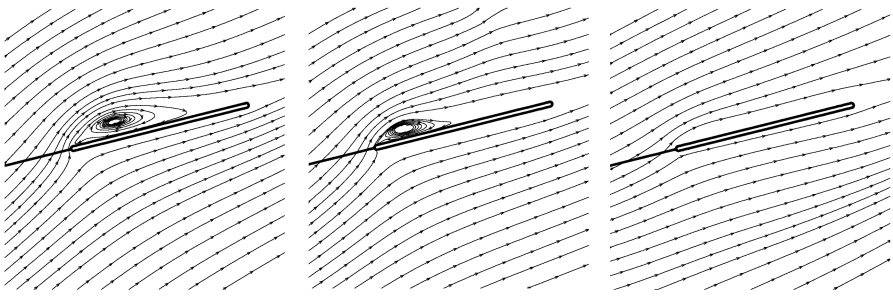

Fig. 4 Streamline plots: a) single wing; b) hindwing at $\gamma_d = 90$ deg; and c) hindwing at $\gamma_d = -90$ deg.

E in Fig. 5c), the flow is only slightly disturbed with respect to the incoming stream; while above the wing (e.g., at points A and B in Fig. 5c and at points A, B, C, and D in Figs. 5d–5f), the flow is turned downward by a large angle (i.e., a downward "jet" or downwash flow is superposed on the incoming flow).

When γ_d is positive (the hindwing leads the forewing), the hindwing in its downstroke would be "below" the forewing and move in a flow that is only slightly disturbed by the forewing, resulting in the small interaction effects. For example, in the case of $\gamma_d = 90$ deg, at $\hat{\tau} = 0$, the point on the chord of the hindwing that is a quarter chord from its leading edge would be at point C in Fig. 5a, where the flow is only slightly disturbed by the forewing. When γ_d is negative (the hindwing lags the forewing), the hindwing in its downstroke would be "below" the forewing and move in the large downwash flow produced by the forewing, reducing its effective angle of attack, hence its aerodynamic force. For example, in the case of $\gamma_d = -90$ deg, at $\hat{\tau} = 0.5$ the point on the chord of the hindwing that is a quarter chord from its leading edge would be at point C in Fig. 5e, where a large downwash flow exists.

IV. Conclusions

At positive γ_d (hindwing leads forewing), the mean total vertical force and mean total thrust of the fore- and hindwings are only slightly influenced by the forewing–hindwing interaction, while at negative γ_d (hindwing lags forewing), the forces, especially the mean total vertical force, are greatly decreased, compared with the case without interaction. The reason for the large decreases in the forces at negative γ_d is as follows: the forewing in each of its downstroke produces a downward "jet" behind it; when the hindwing lags the forewing, it moves in the jet and its effective angle of attack is greatly reduced, resulting in a large decrease in its aerodynamic force; this causes the decreases in the total vertical force and thrust. The present results might explain why dragonflies have been observed only to use positive phase differences in their flight.

References

[1] Freymuth, P., "Thrust Generation by an Airfoil in Hover Modes," *Experiments in Fluids*, Vol. 9, No. 1, 1990, pp. 17–24.

[2] Wang, Z. J., "Two Dimensional Mechanism for Insect Hovering," *Physical Review Letters*, Vol. 85, No. 10, 2000, pp. 2216–2219.

[3] Sun, M., and Lan, S. L., "A Computational Study of the Aerodynamic Forces and Power Requirements of Dragonfly (Aeschna Juncea) Hovering," *Journal of Experimental Biology*, Vol. 207, No. 11, 2004, pp. 1887–1901.

[4] Maybury, W. J., and Lehmann, F., "The Fluid Dynamics of Flight Control by Kinematic Phase Lag Variation Between Two Robotic Insect Wings," *Journal of Experimental Biology*, Vol. 207, No. 26, 2004, pp. 4707–4726.

[5] Yamamoto, M., and Isogai, K., "Measurement of Fluid Dynamic Forces for a Mechanical Dragonfly Model," *AIAA Journal*, Vol. 43, No. 12, 2006, pp. 2475–2480.

[6] Wang, J. K., and Sun, M., "A Computational Study of the Aerodynamics and Forewing–Hindwing Interaction of a Model Dragonfly in Forward Flight," *Journal of Experimental Biology*, Vol. 208, No. 19, 2005, pp. 3785–3804.

[7] Norberg, R. A., "The Pterostigma of Insect Wings and Inertial Regulator of Wing Pitch," *Journal of Comparative Physiology*, Vol. 81, No. 1, 1972, pp. 9–22.

[8] Sun, M., and Yu, X., "Aerodynamic Force Generation in Hovering Flight in a Tiny Insect," *AIAA Journal*, Vol. 44, No. 7, 2006, pp. 1532–1540.

Z. Wang
Associate Editor